Self-calibrated global rainbow refractometry: a dual-wavelength approach

Xuecheng Wu (吴学成)[1,*], Haoyu Jiang (姜淏予)[1], Kailin Cao (操凯霖)[1], Yingchun Wu (吴迎春)[1,2], Can Li (李 灿)[1], Gérard Gréhan[2], Sawitree Saengkaew[2], and Kefa Cen (岑可法)[1]

[1]*State Key Lab of Clean Energy Utilization, Zhejiang University, Hangzhou 310027, China*
[2]*CNRS UMR 6614/CORIA, Saint Etienne du Rouvray BP12 76801, France*
**Corresponding author: wuxch@zju.edu.cn*

Received November 24, 2016; accepted January 13, 2017; posted online February 14, 2017

Calibration of the relationship between the scattering angle and the CCD pixel is a key part of achieving accurate measurements of rainbow refractometry. A novel self-calibrated global rainbow refractometry system based on illumination by two lasers of different wavelengths is proposed. The angular calibration and refractive index measurement of two wavelengths can be completed simultaneously without extra measurement devices. The numerical and experimental results show the feasibility and high precision of the self-calibration method, which enables the rainbow refractometry to be implemented in a more powerful and convenient way. The self-calibrated rainbow system is successfully applied to measure the refractive indices of ethanol-water solutions with volume concentrations of 10% to 60%.

OCIS codes: 290.5820, 120.4820, 120.6780, 290.5820, 290.3030.
doi: 10.3788/COL201715.042902.

Liquid atomization and spray have a broad range of applications in energy, chemical, and many other industrial fields. Accurate measurements and control of the key parameters of droplets in the complex atomization or a spray flow field play an instructive role in mechanism studies of multiphase flows and in the optimization of specific industrial processes. Among the advanced optical measurement techniques[1–4] for characterizing droplets, rainbow refractometry[5–7] has been shown to be a powerful tool for its advantages in simultaneously measuring the size/size distribution (individual droplet/polydispersed droplet cloud) and refractive index. Thereafter, the temperature[8], concentration[9], solution components[10], and other characterization parameters can be determined on the basis of prior knowledge of their relationships with the measured refractive index.

By analyzing the distribution of scattered light around the primary rainbow angle, the rainbow technique extracts the absolute angular location and fits the shape of the rainbow pattern to the inverse of the refractive index and the droplet size. Roth *et al.*[11] first presented the standard rainbow technique (SRT) to measure a single spherical droplet or individual monodispersed droplets in a line. Later, Van Beeck *et al.*[12–14] improved the SRT to the global rainbow technique (GRT) for measuring spray droplets. GRT employs a larger-sized pinhole and longer exposure time of the CCD camera than SRT to get the superposition of the rainbows from numerous droplets that are illuminated by a laser. This superposition of rainbows suppresses the effects of the non-sphericity of the droplets and eliminates the high-frequency ripple component of the rainbow signals to obtain a steady and smooth Airy rainbow structure. Recently, Wu *et al.*[15] proposed a one-dimensional rainbow technique (ORT-1) that extended a point volume measurement to a one-dimensional segment measurement by using slit apertures. Then, Wu *et al.*[16] developed an alternative optical design of the one-dimensional rainbow technique (ORT-2) which aims to facilitate the angular calibration in the full image field by using Fourier domain filtering.

Since the information on the refractive index contained in the rainbow intensity distribution is highly sensitive to the scattering angle, precise calibration of the relationship between the scattering angle (θ) and the CCD pixel (pix) is the key part of guaranteeing the measurement accuracy. One of the calibration methods involves acquiring global rainbow images of a set of sprays with known temperatures[17], but it is susceptible to environmental perturbations, such as temperature changes. The calibration process usually involves rotating a mirror mounted in the measurement volume[18,19], which we call the mirror calibration method. However, errors caused by manual operation and additional precision instruments are unavoidable in the mirror calibration method. When it comes to harsh industrial environments, such as sprays in containers, the calibration of the mirror in inaccessible occasions represents a challenge. To solve the problem, we propose a self-calibration method based on dual-wavelength lasers for global rainbow refractometry. This method enables us to calibrate the scattering angle along with the refractive index measurement under two wavelength illuminations.

As the material's natural property, the refractive index changes with the wavelength of light, while other conditions remain the same. The refractive indices of common liquids, such as water and alcohol, decrease with the

wavelength. For spray droplets illuminated by two laser beams of different wavelengths that are modulated into a coincident beam, two rainbow patterns of different wavelengths can be drawn from the original polychromatic rainbow pattern by the method of appropriate signal separation. Obviously, these two rainbow patterns correspond to the identical particle size distribution and the temperature. If the equation for the refractive index as a function of the wavelength and temperature is generally known in advance, according to the coupling relationship of the refractive index between this pair of rainbows, both the calibration equation and the droplet temperature (T) might be yielded simultaneously.

The typical dual-wavelength global rainbow curves with identical particle size distributions and temperatures have the same curve shape and different positions on the horizontal axis, which correspond, respectively, to the same size distribution and different refractive indices due to the two wavelengths, as shown in Fig. 1(a). Global rainbow curves are simulated based on the Lorenz–Mie theory (only used as the simulation method described by Wu *et al.*[9]). Pix_1 and pix_2 are the positions of the rainbows corresponding to the geometric rainbow angles θ_{rg1} and θ_{rg2} and can be determined by the angles where the normalized scattering light intensities reach a value of R_I ($R_I = I_{rg}/I_{\mathrm{MAX}}$) before the primary rainbow maximum, which is related to the droplet size. I_{rg} is the scattered light intensity at the geometric rainbow angle. I_{MAX} is the scattered light intensity that reaches the maximum. The geometric rainbow angle θ_{rg} only depends on the refractive index (n), which varies with the wavelength of light and is given by[20]

$$\boldsymbol{\theta}_{rg} = 2\arccos\left[\frac{1}{n^2}\left(\frac{4-n^2}{3}\right)\right]^{3/2}. \tag{1}$$

The equation for the refractive index of the sprayed droplet as a function of the wavelength and temperature should be known in advance, so here we choose deionized water, whose physical characteristics have been fully studied, as given by[21]

$$n(T,\lambda) = 1.31405 - 2.02\times10^{-6}T^2 + (15.868 - 0.00423T)\lambda^{-1} - 4382\lambda^{-2} + 1.1455\times10^{6}\lambda^{-3}. \tag{2}$$

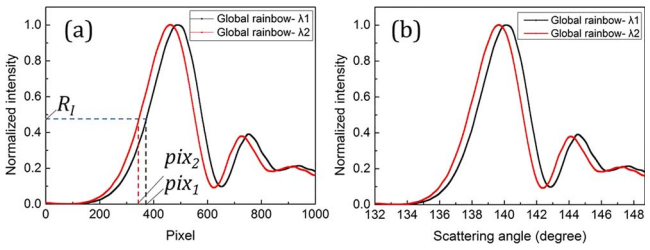

Fig. 1. Typical global rainbow curves under two wavelengths: (a) distributions of the light intensity on the pixel number and (b) distributions of the light intensity on the scattering angle by calibration.

When the spray temperature (T) has been hypothesized, the refractive indices of the calibration medium under two wavelengths (n_1, n_2) can be determined by Eq. (2), and the geometric rainbow angles can be calculated by Eq. (1).

Since the calibrated angle-pixel relationship in the paraxial rainbow imaging system presents good linearity between the scattering angle θ and the CCD pixel, the calibration equation is usually obtained by linear fitting ($\theta = a + b \times \mathrm{pix}$) the dispersed calibration points in the classical mirror calibration method and has been shown to ensure accuracy[9,17–19]. By hypothesizing the values of R_I and the spray temperature T, two characteristic calibration points $(\mathrm{pix}_1, \theta_{rg1})$ and $(\mathrm{pix}_2, \theta_{rg2})$ can be used to obtain the linear calibration equation. Then, we get the dual-wavelength distributions of the intensity on the scattering angle, as shown in Fig. 1(b). These distributions are utilized for the rainbow signal processing to inverse the refractive indices (m_1, m_2) by using an inversion algorithm based on the modified Nussenzveig's theory[22]. This inversion algorithm was proposed by Saengkaew *et al.*[23]. Using the non-negative least-squares algorithm, the refractive indices (m_1, m_2) and the identical size distribution can be inversed, respectively, by solving

$$\vec{I}_1(\theta) = \vec{T}_1(m_1, d, \theta)\vec{D}(d), \tag{3}$$

$$\vec{I}_2(\theta) = \vec{T}_2(m_2, d, \theta)\vec{D}(d). \tag{4}$$

The intensity vector $\boldsymbol{I}$ is the scattered light intensity distribution extracted from the CCD recordings. The rainbow scattering coefficient matrix $\boldsymbol{T}$ is computed by using the modified Nussenzveig's theory, and the vector $\boldsymbol{D}$ is the size distribution of the spray droplets. The subscripts 1 and 2 correspond to λ_1 and λ_2, respectively.

For a particular spray, its actual refractive indices under two wavelengths are definitely certain values. Any deviation either in the preset value of R_I or the preset temperature T would result in an error when comparing the inverse refractive indices (m_1, m_2) with the hypothesizing refractive indices (n_1, n_2). Thus, the actual refractive indices of the droplets under two wavelengths and the calibration equation can be obtained simultaneously by searching the minimum of the root mean square (RMS) errors between the hypothesizing refractive indices and the ones from the inversion. A typical example shows the RMS error for the case of a deionized water spray at 25°C under two wavelengths ($\lambda_1 = 532$ nm, $\lambda_2 = 632.8$ nm) with the actual value of R_I 0.47, as shown in Fig. 2.

The actual refractive indices of deionized water under two wavelengths at each temperature can be calculated by Eq. (2). Tested sprays at temperatures ranging from 20°C–30°C and R_I ranging from 0.44–0.49 are inspected. The preset value of R_I and the preset spray temperature T are used to obtain the hypothesizing refractive indices (n_1, n_2) and linear calibration equation, which can be used to inverse the refractive indices (m_1, m_2) from the simulated global rainbow curves. The result in Fig. 2 shows that the RMS error between the inverse refractive indices

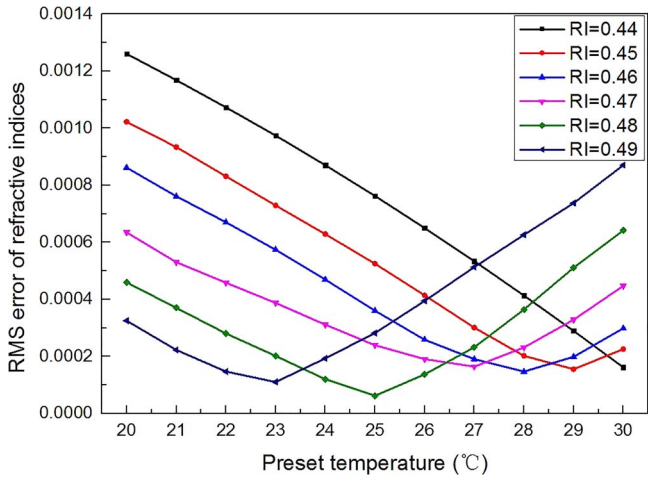

Fig. 2. Simulated RMS errors between the preset refractive indices and the ones from the rainbow signal inversion with different preset values of R_I and a preset temperature for the deionized water spray under two wavelengths (532 and 632.8 nm) at 25°C ($R_I = 0.47$).

(m_1, m_2) and the preset refractive indices (n_1, n_2) is significantly decreased when the tested temperature and the value of R_I are close to the target ones. By iteratively searching for the minimum error, the temperature, R_I and the calibration equation can be obtained at the same time.

The feasibility of the self-calibration method presented above is demonstrated by the experimental setup in Fig. 3. A vertically emitted semiconductor laser (wavelength: $\lambda_1 = 532$ nm) and an He–Ne laser (wavelength: $\lambda_2 = 632.8$ nm) are transformed into one coincident laser beam (polarized light) by a 560 nm dichroic beam splitter ($\lambda > 560$ nm transmit; $\lambda < 560$ nm reflect). The backscattered light of the spray illuminated by the coincident laser beam is collected by lens 1 with a diameter of 10 cm and a focal length of 16 cm. Lens 1 is placed 25 cm away from the probe volume. An aperture with a diameter of 2 mm is located at the image plane of the lens 1 in order to select and define the measured probe volume. Then, the collected light passes through an aspherical lens 2 with a diameter of 10 cm and a focal length of 8 cm. Lens 2 conjugates the image focal plane of lens 1 onto the color CCD sensor, which records polychromatic rainbows with a resolution of 1392×1040 pixels (6.45 μm/pixel). A spray of deionized water is tested.

A typical global rainbow image of mixed rainbow signals is shown in Fig. 4(a). Accoring to RGB three-channel spectral response coefficients of the CCD under wavelengths of 532 and 632.8 nm, the dual-wavelength scattered light signals can be separated, as shown in Figs. 4(b) and 4(c).

The distributions of the scattered light intensity separated by the wavelengths of 532 and 632.8 nm are shown in Fig. 5. The value of $R_I = 0.45$ and the temperature $T = 23$°C are used as the initial preset values. Depending on the self-calibration method presented above, we can search the minimum of the RMS errors of the preset refractive indices and the ones from the inversion through iterations of correcting the preset R_I and the temperature.

When the iteration is finished, the final preset R_I equals 0.47, and the temperature T equals 20°C. The temperature measured by the self-calibration method is consistent with the thermocouple reading of 21.2°C, which is in the error range (±0.75%) of a k-type thermocouple. Pixels $(\text{pix}_1 = 481, \text{pix}_2 = 445)$ corresponding to the final preset geometric rainbow angles ($\theta_{rg1} = 138.22°$, $\theta_{rg2} = 137.74°$) can be located in the global rainbow curves with the help

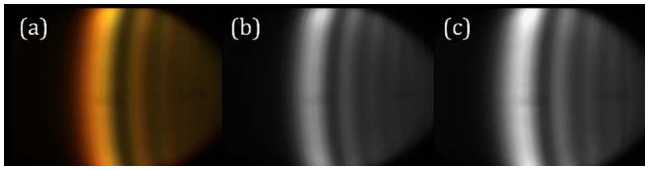

Fig. 4. (a) Original global rainbow image of a spray of deionized water and images of separated dual-wavelength signals under the wavelengths of (b) 532 and (c) 632.8 nm.

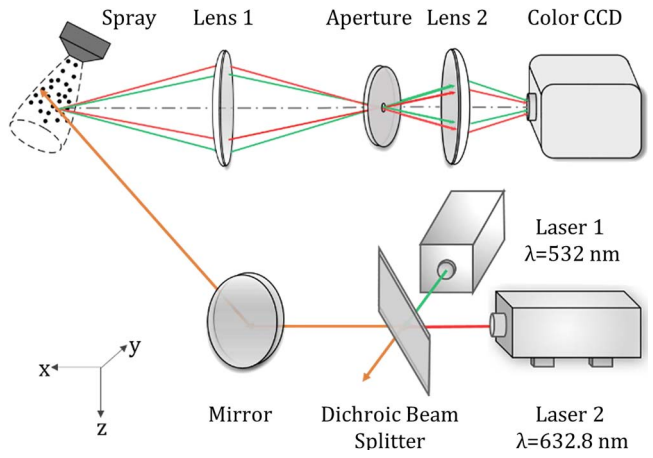

Fig. 3. Optical setup of the self-calibrated global rainbow system.

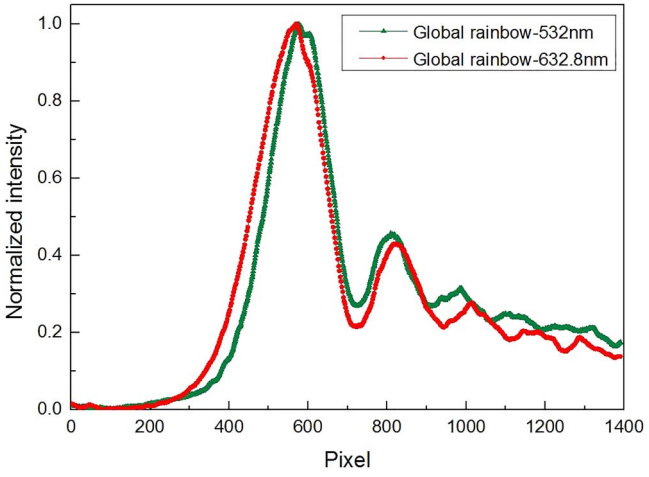

Fig. 5. Global rainbow curves of a spray of deionized water: dual-wavelength distributions of scattered light intensity.

of the value of R_I. Two characteristic calibration points, $(\mathrm{pix}_1, \theta_{rg1})$ and $(\mathrm{pix}_2, \theta_{rg2})$, can be used to obtain the parameters of a linear calibration equation, $a = 131.81°$ and $b = 0.01333°$/pixel. The final RMS error equals 9.1×10^{-5} by comparing the preset refractive indices ($n_1 = 1.33504, n_2 = 1.33176$) at 20°C and the ones from the inversion ($m_1 = 1.33513, m_2 = 1.33184$).

The performance of this self-calibrated global rainbow system is tested and verified further by ethanol-water solutions with volume concentrations from 10% to 60%. Figure 6 shows polychromatic global rainbow images of the ethanol-water solutions. The location of the bright fringe in the rainbow image shifts to the right distinctly, which means the refractive index increases with the volume concentration in the range of 10% to 60%.

The refractive indices of the ethanol-water solutions were directly inversed from the separated dual-wavelength signals. The results measured using the self-calibration method and the mirror calibration method are illustrated in Fig. 7. The measurement results of these two calibration methods, shown by solid (self-calibration) and dashed (mirror calibration) curves, fit well under the two

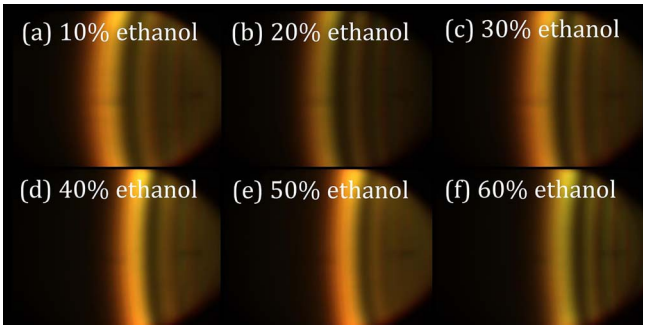

Fig. 6. Polychromatic global rainbow images of ethanol-water solutions with volume concentrations from 10% to 60% in steps of 10%.

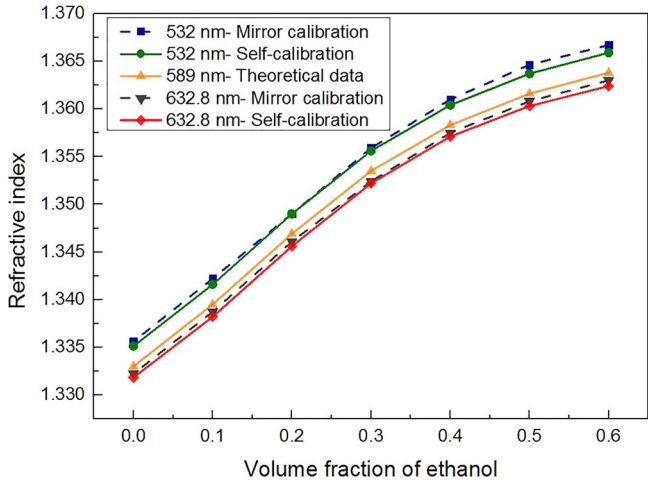

Fig. 7. Comparison of the measured refractive index by the methods of mirror calibration and self-calibration with the theoretical data for the ethanol-water solutions at 20°C.

wavelengths. Figure 7 shows that the average discrepancy of the refractive index between the two calibration methods is 0.0005, which is equivalent to a discrepancy of the scattering angle of ~0.07°. This difference might be caused by the instrumental uncertainty of the rotating platform under the mirror (rotating accuracy: 0.05°) and the positioning deviation of the geometric rainbow angles due to the residual noise in the filtered rainbow curves (positioning deviation: ~0.03°). Also, these inversion results show good agreement with the reported values[24]. For the methods of self-calibration and mirror calibration, the average deviations of the refractive index under each of the two adjacent wavelengths (532, 589, 589, and 632.8 nm) are 0.00198 and 0.00146, which are both roughly in line with the average wavelength deviation of 0.00212 at 20°C calculated by Eq. (2). But obviously, this deviation of the self-calibration method comes closer to the theoretical calculation than that of the mirror calibration method. This indicates that the self-calibration method yields a higher precision than the mirror calibration method.

Note that to obtain both the calibration equation and the refractive index under two wavelengths, this self-calibrated system only works for liquids for which the refractive index is a known function of the wavelength and temperature. In other words, liquids whose physical parameters have been fully studied, such as deionized water, can be used as a calibration medium to complete the angular calibration for rainbow refractometry without an additional precise measurement device for the angle, temperature, or refractive index.

In conclusion, by use of the natural shift of a rainbow pattern under two wavelengths, the relationship between the scattering angle and the CCD pixel is calibrated, along with the measurement of the refractive indices under two wavelengths. We call this method self-calibrated global rainbow refractometry. The feasibility of the self-calibration method is tested by simulations and experiments, and the results show that it is an efficient and accurate calibration method for a global rainbow system. This method spares the rainbow refractometry from extra angle or temperature measuring instruments. It enables rainbow refractometry to be implemented in a more powerful and convenient way, and it may even be extended to calibration for the one-dimensional rainbow technique.

This work was supported by the National Natural Science Foundation of China (No. 51576177), the Major Program of the National Natural Science Foundation of China (No. 51390491), the National Basic Research Program of China (No. 2015CB251501), and the Program of Introducing Talents of Discipline to University (No. B08026).

References

1. Z. Kuang, L. Cheng, Y. Liang, H. Liang, and B. Guan, Chin. Opt. Lett. **14**, 050602 (2016).

2. Y. Liu, R. Li, X. Lan, Z. Shen, J. Lu, and X. Ni, Chin. Opt. Lett. **3**, 88 (2005).
3. L. Yao, X. Wu, J. Yang, Y. Wu, X. Gao, L. Chen, G. Gréhan, and K. Cen, Chin. Opt. Lett. **13**, 072801 (2015).
4. Z. Qi, J. Yao, L. Zhao, Y. Cui, and C. Lu, Photon. Res. **3**, 313 (2015).
5. C. Letty, B. Renou, J. Reveillon, S. Saengkaew, and G. Gréhan, Combust. Flame **160**, 1803 (2013).
6. M. Ouboukhlik, G. Godard, S. Saengkaew, M. C. F. Salaün, L. Estel, and G. Gréhan, Chem. Eng. Technol. **38**, 1154 (2015).
7. E. Porcheron, P. Lemaitre, A. Nuboer, V. Rochas, and J. Vendel, Nucl. Eng. Des. **237**, 1862 (2007).
8. J. Hom and N. Chigier, Appl. Opt. **41**, 1899 (2002).
9. X. Wu, Y. Wu, S. Saengkaew, S. Meunier-Guttin-Cluzel, G. Gréhan, L. Chen, and K. Cen, Meas. Sci. Technol **23**, 125302 (2012).
10. Y. Zhao and H. H. Qiu, Exp. Fluids **40**, 60 (2006).
11. N. Roth, K. Anders, and A. Frohn, Appl. Opt. **30**, 4960 (1991).
12. J. Van Beeck, D. Giannoulis, L. Zimmer, and M. L. Riethmuller, Opt. Lett. **24**, 1696 (1999).
13. M. R. Vetrano, J. P. Antonius Johannes Van Beeck, and M. L. Riethmuller, Opt. Lett. **30**, 658 (2005).
14. J. P. van Beeck, L. Zimmer, and M. L. Riethmuller, Part. Part. Syst. Charact. **18**, 196 (2001).
15. X. Wu, H. Jiang, Y. Wu, J. Song, G. Gréhan, S. Saengkaew, L. Chen, X. Gao, and K. Cen, Opt. Lett. **39**, 638 (2014).
16. Y. Wu, J. Promvongsa, X. Wu, K. Cen, G. Grehan, and S. Saengkaew, Opt. Express **23**, 30545 (2015).
17. P. Lemaitre, E. Porcheron, G. Gréhan, and L. Bouilloux, Meas. Sci. Technol **17**, 1299 (2006).
18. J. Wilms and B. Weigand, Appl. Opt. **46**, 2109 (2007).
19. M. R. Vetrano, S. Gauthier, J. van Beeck, P. Boulet, and J. Buchlin, Exp. Fluids **40**, 15 (2006).
20. J. A. Adam, Appl. Opt. **47**, H11 (2008).
21. X. Quan and E. S. Fry, Appl. Opt. **34**, 3477 (1995).
22. H. M. Nussenzveig, J. Opt. Soc. Am. **69**, 1068 (1979).
23. S. Saengkaew, T. Charinpanikul, C. Laurent, Y. Biscos, G. Lavergne, G. Gouesbet, and G. Gréhan, Exp. Fluids **48**, 111 (2010).
24. E. E. Hall and A. R. Payne, Phys. Rev. **20**, 249 (1922).